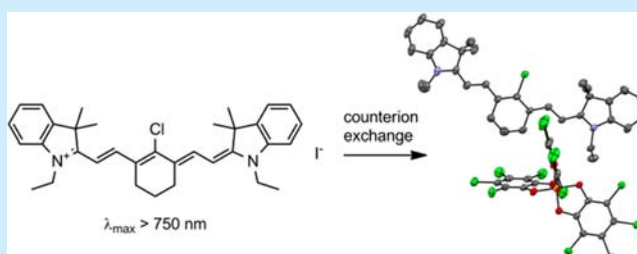


## NIR-Absorbing Heptamethine Dyes with Tailor-Made Counterions for Application in Light to Energy Conversion

Anna C. Véron,<sup>\*,†,‡</sup> Hui Zhang,<sup>†</sup> Anthony Linden,<sup>‡</sup> Frank Nüesch,<sup>†</sup> Jakob Heier,<sup>†</sup> Roland Hany,<sup>†</sup> and Thomas Geiger<sup>\*,†</sup><sup>†</sup>Laboratory for Functional Polymers, Swiss Federal Laboratories for Materials Science and Technology (Empa), 8600 Dübendorf, Switzerland<sup>‡</sup>University of Zurich (UZH), Department of Chemistry, 8057 Zürich, Switzerland

## Supporting Information

**ABSTRACT:** A method to exchange the counterion of cyanine dyes to  $\Delta$ -TRISPHAT<sup>−</sup> and PF<sub>6</sub><sup>−</sup> is presented. The influence of these counterions on the photophysical and electrochemical properties of the cyanine dye in solution is discussed, and tendencies in the solid packing are highlighted by X-ray crystal structures. The compounds were applied in semitransparent bilayer organic solar cells together with C<sub>60</sub>, and a power conversion efficiency of 2.2% was achieved while maintaining a high transparency level in the visible region of 66%.



Organic dyes that absorb in the near-infrared (NIR) region are finding interest in different applications in organic electronics, such as for light-to-energy conversion in organic photovoltaic (OPV) cells. The synthesis and analysis of new NIR dyes is of importance for further development of OPV technology; strong NIR absorbers not only allow more low energy photons to be harvested, as is required for multijunction cells, for example, but also permit (semi)transparent solar cells with high visible light transparency to be produced. Many dyes are known that have several or broad absorption bands, tailing into the NIR region.<sup>1</sup> However, the possibilities for achieving chromophores with a single sharp absorption maximum ( $\lambda_{\text{max}}$ ) above 750 nm are limited. Dyes with that feature can be found, among others, in the classes of squaraine dyes, croconian dyes, and polymethine dyes. Polymethine dyes are known for their outstanding optical properties, such as tunable absorption maximum ( $\lambda_{\text{max}}$ ) by elongation of the methine chain and high molar extinction coefficients ( $\epsilon > 10^5 \text{ M}^{-1} \text{ cm}^{-1}$ ). Additionally, their redox potentials are suitable for electron transfer to fullerenes,<sup>2</sup> which are ubiquitous electron acceptors in OPV cells. Polymethine dyes have been shown to be useful candidates for applications in dye-sensitized solar cells (DSSCs)<sup>3</sup> as well as in OPV cells.<sup>4</sup> The focus in this paper is on heptamethine dyes, which exhibit  $\lambda_{\text{max}} \geq 750 \text{ nm}$ ,  $\epsilon > 3 \times 10^5 \text{ M}^{-1} \text{ cm}^{-1}$ , and on their application in semitransparent OPV cells.

Polymethine dyes are cationic, and their properties can be tuned not only by structural modification of the dye core but also by the choice of counterion. The presence of mobile ions has been found to be beneficial for the performance of organic semiconductor devices such as organic solar cells.<sup>5</sup> Bouit et al. have intensively investigated the influence of different counter-

ions on the photophysical properties of heptamethine dyes.<sup>6</sup> Small, hard counterions polarize the cationic dye core, leading to a bond length alteration (BLA) and disruption of the ideal polymethine state (IPS),<sup>6</sup> which is manifested as a blue shift of  $\lambda_{\text{max}}$  and a decreased  $\epsilon$ . They could show that soft, bulky anions, such as the TRISPHAT<sup>−</sup> anion,<sup>7</sup> are the most suitable for reaching IPS.

The PF<sub>6</sub><sup>−</sup> counterion has previously been used for cyanine dyes in OPV applications, mainly via trimethine cyanine PF<sub>6</sub><sup>−</sup> salts,<sup>8</sup> which are commercially available. To our knowledge, cyanines with TRISPHAT<sup>−</sup> as the counterion have not been studied in solar cell applications so far. We speculated that the aromatic moieties of the TRISPHAT<sup>−</sup> anion could result in a favorable interaction between the cyanine salt and C<sub>60</sub> at the heterojunction, resulting in improved OPV cell performance.<sup>9</sup>

In this study, we present fast and easy methods for the counterion exchange of heptamethine dyes from I<sup>−</sup> to PF<sub>6</sub><sup>−</sup> and TRISPHAT<sup>−</sup>. Compounds 1 and 2 (Figure 1) have been prepared in high purity and were fully characterized (see the Supporting Information). We investigate the influence of the counterion on the optical and electrochemical properties, crystal structure, and finally, the performance of bilayer organic solar cells.

Synthesis of the heptamethine dye core was achieved via Knoevenagel condensation reaction of an alkylated indole precursor with an activated methyl group (S1, see the Supporting Information) and a dianil compound carrying the central cyclohexene moiety (S2).<sup>10</sup> The reaction was carried out in ethanol under dry conditions, using sodium acetate as a

Received: November 28, 2013

Published: February 5, 2014

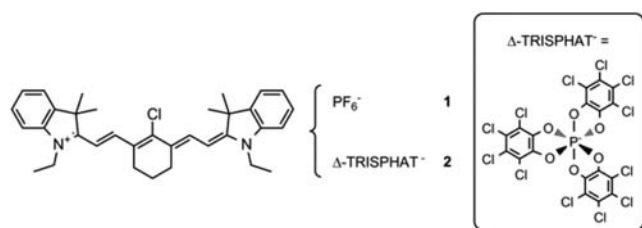
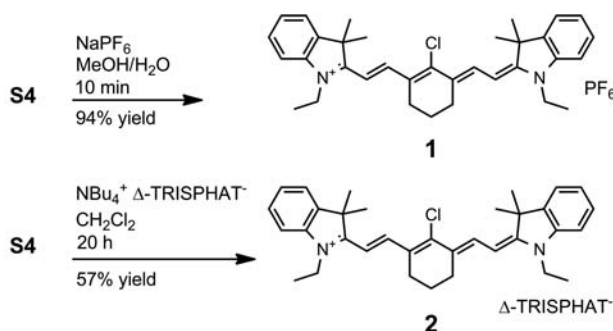


**Figure 1.** Structure of the heptamethine cation with the counterions hexafluorophosphate and TRISPHAT<sup>−</sup>.

catalyst. Ion-exchange reactions were carried out using the iodide salt of the heptamethine dye (**S4**). In order to exchange I<sup>−</sup> for PF<sub>6</sub><sup>−</sup>, sodium hexafluorophosphate (NaPF<sub>6</sub>) was added to a solution of **S4**, leading to precipitation of salt **1**.<sup>6</sup> Exchange from I<sup>−</sup> to Δ-TRISPHAT<sup>−</sup> was carried out by stirring a solution of **S4** and NBu<sub>4</sub><sup>+</sup> TRISPHAT<sup>−</sup> (**S3**) in DCM overnight (Scheme 1). First, purification was achieved by column

#### Scheme 1. Ion-Exchange Reactions



**S4** = iodide salt of the heptamethine cation. For details see Supporting Information.

chromatography. Then, both products **1** and **2** were recrystallized from appropriate solvents to give salts of high purity, confirmed by elemental analysis and NMR data. Synthetic details of all compounds and precursors are given in the Supporting Information.

UV–vis absorption spectra of the compounds in solution have been recorded in different solvents, and their molar extinction coefficients, integrated absorption coefficients (IAC),<sup>11</sup> and oscillator strengths were calculated. Absorption spectra of the dyes in different solvents are shown in Figure 2, a summary of the optical properties in chlorobenzene is given in Table 1, and a more detailed overview with values from different solvents is provided in the Supporting Information (Table S3.1). The heptamethine dyes show a narrow absorption band between 650 and 850 nm. The value of  $\lambda_{\text{max}}$  is equal for **1** and **2** in each solvent, suggesting that the ions dissociate in solution and the absorption of the dye cation is not influenced by the anions. With decreasing polarity of the solvent,<sup>12</sup> a slight bathochromic shift of  $\lambda_{\text{max}}$  can be observed (positive solvatochromism). However, the change in  $\lambda_{\text{max}}$  is so small that it can be assumed that the nature of the ground state and excited state remain similar. The solvent has an influence on  $\epsilon$  as well as on the peak shape. In the case of **2**, extraordinarily high values for  $\epsilon$  are found in the chlorinated solvents chloroform and chlorobenzene (375000 and 360000, respectively, compared to an average value of 240000 M<sup>−1</sup> cm<sup>−1</sup> in the other solvents). When comparing the IAC, however, it can be seen that the area under the absorption band is very

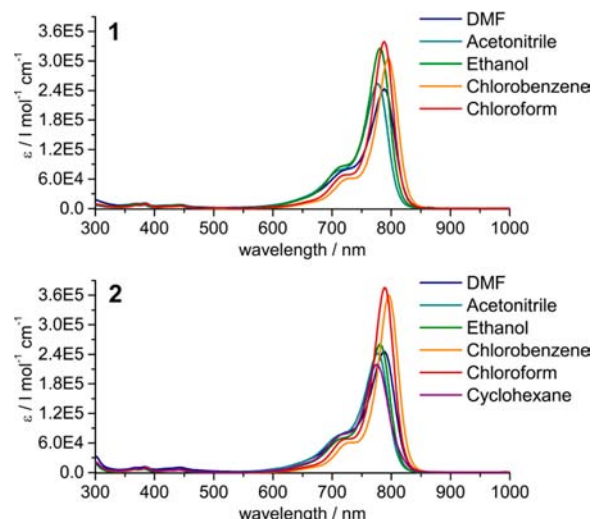


**Figure 2.** Absorption spectra of the dyes in different solvents normalized to their molar extinction coefficients at  $\lambda_{\text{max}}$ .

**Table 1.** Optical Properties of **1** and **2** in Chlorobenzene

dye	$\lambda_{\text{max}}^a$ (nm)	$\epsilon^b$ (M <sup>−1</sup> cm <sup>−1</sup> )	IAC × 10 <sup>18c</sup> (M <sup>−1</sup> cm <sup>−1</sup> s <sup>−1</sup> )	$f^d$
<b>1</b>	795	305000	9.16	1.32
<b>2</b>	796	360000	9.81	1.41

<sup>a</sup>Absorption maximum. <sup>b</sup>Molar extinction coefficient at  $\lambda_{\text{max}}$ . <sup>c</sup>Integrated absorption coefficient. <sup>d</sup>Oscillator strength. For details about the determination of these values, see the Supporting Information.

similar ( $9 \times 10^{18}$  to  $1 \times 10^{19}$  M<sup>−1</sup> cm<sup>−1</sup> s<sup>−1</sup> in all solvents), indicating an absorption of similar intensity in all solvents. The difference in  $\epsilon$  arises from much narrower peak shapes in the chlorinated solvents. This could be due to a better solubilization of the dyes in these solvents, leading to less dimerization/aggregation.

Absorption spectra of thin films (20 nm) on glass substrates spin-coated from chlorobenzene are shown in Figure 5. In contrast to the spectra in solution, the counterion has an effect on the absorption in the solid state. Compound **1** has a broader absorption band than **2**, which indicates a stronger tendency to aggregate in the case where PF<sub>6</sub><sup>−</sup> is chosen as the counterion.

CV measurements were carried out in DMF solution to determine the redox potentials of the dyes (details are described in the Supporting Information). It was found that the counterion does not have an influence on the electrochemical properties of the cation. For both **1** and **2**, the oxidation potential vs vacuum  $E_{\text{ox}}^0$  was found to be −5.37 eV, and the reduction potential  $E_{\text{red}}^0$  was at −4.20 eV. The electrochemical band gap is 1.17 eV. The counterions themselves are not redox active in the potential range of the cation or C<sub>60</sub>, which is beneficial for their application in solar cells as the electrons cannot be trapped by the counterions.

Single crystals of **1** and **2** suitable for X-ray crystal structure analysis could be grown by vapor diffusion of Et<sub>2</sub>O into DCM solutions of each compound. The packing of the cations in the crystal structures is influenced to a large extent by the counterion.

With the PF<sub>6</sub><sup>−</sup> counterion (compound **1**) a monoclinic solvent-free crystal structure in the space group *Pn* was obtained. The asymmetric unit (Figure 3a) contains four

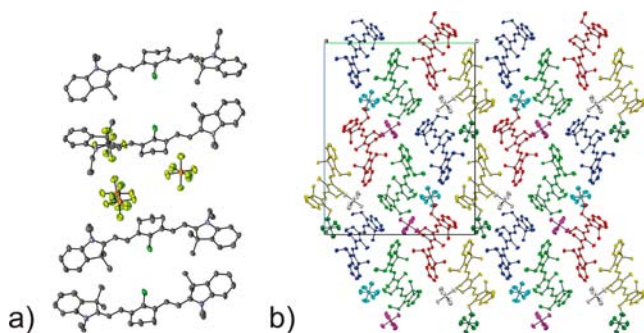


**Figure 3.** Crystal structure of **1**: (a) asymmetric unit, (b) crystal packing viewed along the *a*-axis, colored by symmetry equivalence.

symmetry-independent cations and anions. The independent cations generally have very similar conformations with only small differences in most torsion angles. The major differences are that one cation has the terminal methyl group of one ethyl substituent rotated by approximately 180° relative to its orientation in the other three cations and that another cation has the opposite half-chair puckering of the central six-membered ring compared with the other cations. No additional crystallographic symmetry could be found in the structure, although the structure is pseudocentrosymmetric with an 83% fit of the atoms to the additional symmetry element; the differences between the conformations of the cations are breaking the additional symmetry. No obvious interactions, such as  $\pi$ – $\pi$  stacking, could be found (Figure 3b).

With  $\Delta$ -TRISPHAT<sup>−</sup> as the counterion (compound **2**), a triclinic crystal structure in the space group  $P\bar{1}$  was obtained. In contrast to the structure with PF<sub>6</sub><sup>−</sup>, only one cation and anion is found in the asymmetric unit alongside some highly disordered solvent molecules which are assumed to be diethyl ether (Figure 4a). In the crystal packing (Figure 4b), the

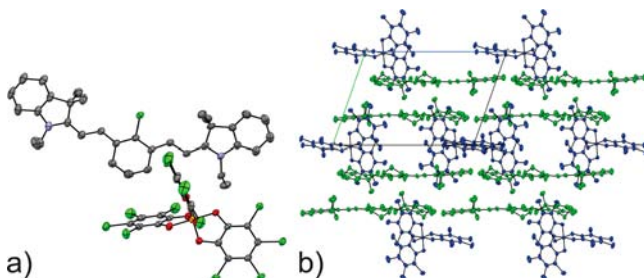


**Figure 4.** Crystal structure of **2**: (a) asymmetric unit, (b) crystal packing viewed along the *b*-axis, colored by symmetry equivalence.

cations and anions form layers parallel to the *a*-axis. However, the distances between the  $\pi$ -systems of the cyanine cations are on the order of 10 Å, and thus no  $\pi$ – $\pi$  stacking occurs. More details about the X-ray crystal structure determination and refinement can be found in the Supporting Information.

Bilayer organic solar cells were fabricated with **1** or **2** as the electron donor and C<sub>60</sub> as the electron acceptor. The cathode was either composed of an 80 nm thick reflective Ag layer; alternatively, semitransparent cells were fabricated with an Ag (12 nm)/Alq<sub>3</sub> (60 nm) electron-collecting electrode (Figure 5b). Therefore, highly transparent devices were obtained with average (450–670 nm) visible transmittance values of 62% (for **1**) and 66% (for **2**) and maximum transparencies of over 75% (Figure 5a).<sup>14</sup> For semitransparent OPV cells, best perform-

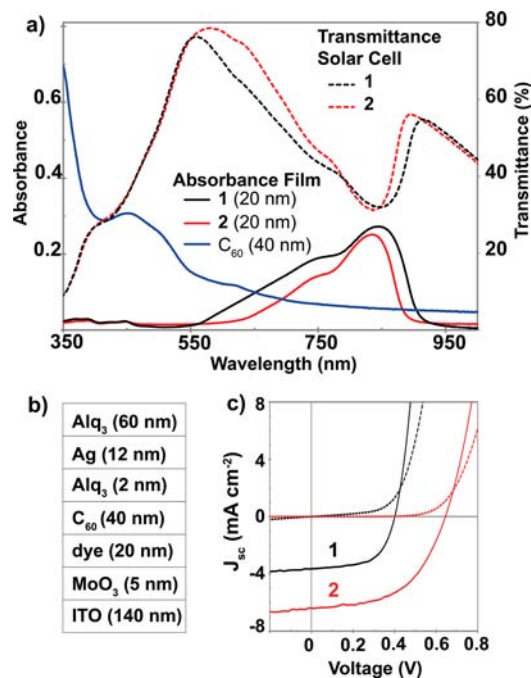


**Figure 5.** (a) Absorbance spectra of thin films of C<sub>60</sub>, **1**, and **2**; transmittance spectra of solar cells. (b) Schematic of the optimized semitransparent cyanine/C<sub>60</sub> cell architecture. (c) White light (solid lines) and dark (dotted lines) solar cell *J*–*V* characteristics for solar cells with **1** (black) and **2** (red).

ances were (for **1**)  $J_{sc} = 3.6 \text{ mA cm}^{-2}$ ,  $V_{oc} = 0.38 \text{ V}$ , FF = 64.8%,  $\eta = 0.9\%$  and (for **2**)  $J_{sc} = 6.4 \text{ mA cm}^{-2}$ ,  $V_{oc} = 0.63 \text{ V}$ , FF = 54.0%,  $\eta = 2.2\%$  (Figure 5c).<sup>15</sup> For nontransparent devices,  $\eta = 1.8\%$  for **1** and  $\eta = 2.8\%$  for **2** were measured. In general, semitransparent devices have a lower performance compared to devices that use a highly reflective back metal contact. Average performance values are given in the Supporting Information.

The influence of the counterion on solar cell performance is notable. The decreased  $J_{sc}$  for **1**, despite its broader absorption spectrum (Figure 5a), indicates a lower charge generation yield at the dye/C<sub>60</sub> heterojunction. Also,  $V_{oc}$  for **1** is considerably lower as compared to **2**. It has been shown that  $V_{oc}$  is correlated to the redox energy levels of the active donor and acceptor materials,<sup>16</sup> and specific factors have been identified that limit  $V_{oc}$ , such as morphology, bimolecular charge recombination, or shunt conduction.<sup>17</sup> Indeed, reverse dark current densities for cells using **1** ( $-2 \text{ mA cm}^{-2}$  at  $-1 \text{ V}$ ) were considerably higher than for **2** ( $-0.04 \text{ mA cm}^{-2}$ ), resulting in a lowered  $V_{oc}$  and eroding the device efficiency partly.

In ongoing work, we also consider that the packing of the ions in the film, the formation of dipole layers, and potential shifts at the dye/C<sub>60</sub> interface have a strong influence on the energetics of the relevant redox levels. The redox levels as measured by CV in solution are the same for **1** and **2**, and  $E^0_{red}$  ( $-4.20 \text{ eV}$ ) is in principle unfavorable for electron transfer after dye excitation to C<sub>60</sub> ( $E^0_{red} = -3.85 \text{ eV}$  from CV in *o*-dichlorobenzene<sup>14</sup>). Therefore, we must assume that the redox potentials of individual molecules in solution do not reflect the energetic situation in the solid film and hence in the actual OPV cells.

In conclusion, we demonstrated the small effect of different counterions of a cyanine dye on its properties in solution but found that the counterion influences the packing and arrangement of the dyes in the crystalline state substantially.



The influence of the counterion on the X-ray crystal structures is notable; however, these structures do not allow conclusions to be made about the arrangement of dye cations and counterions in the spin-coated films used in solar cells, as they are expected to be amorphous. NIR-absorbing cyanine dyes are a suitable class of small molecules for semitransparent OPV cells, and the proper choice of the dye counterion appears to have a pronounced influence on their performance.

## ■ ASSOCIATED CONTENT

### ■ Supporting Information

Details about the preparation and characterization of the compounds, solar cell fabrication, and crystal structure data (CIF). This material is available free of charge via the Internet at <http://pubs.acs.org>.

## ■ AUTHOR INFORMATION

### Corresponding Authors

\*E-mail: [anna.veron@empa.ch](mailto:anna.veron@empa.ch).

\*E-mail: [thomas.geiger@empa.ch](mailto:thomas.geiger@empa.ch).

### Notes

The authors declare no competing financial interest.

## ■ ACKNOWLEDGMENTS

We thank Laurent Bigler and his team (University of Zurich) for MS spectra, Michael Schneider (ETH Zurich) for elemental analyses, and Beatrice Fischer and Daniel Rentsch (Empa Dübendorf) for thermal analyses and NMR spectroscopy. We also acknowledge Jay S. Siegel (University of Tianjin) for support and discussions, and the Brazilian Swiss Joint Research Programme (BSJRP) for financial support.

## ■ REFERENCES

- (1) (a) Fabian, J.; Nakazumi, H.; Matsuoka, M. *Chem. Rev.* **1992**, *29*, 1197. (b) Tyutyulkov, N.; Fabian, J.; Mehlhorn, A.; Dietz, F.; Tadjer, A. *Polymethine dyes, Structure and Properties*; St. Kliment Ohridski University Press: Sofia, 1991.
- (2) (a) Villegas, C.; Krokos, E.; Bouit, P.-A.; Delgado, J. L.; Guldi, D. M.; Martin, N. *Energy Environ. Sci.* **2011**, *4*, 679. (b) Bouit, P.-A.; Spänig, F.; Kuzmanich, G.; Krokos, E.; Oelsner, C.; Gracia-Garibay, M. A.; Delgado, J. L.; Martin, N.; Guldi, D. M. *Chem.—Eur. J.* **2010**, *16*, 9638.
- (3) (a) For a review on other NIR dyes for DSSC, see: Park, J.; Viscardi, G.; Barolo, C.; Barbero, N. *Chimia* **2013**, *67*, 129. (b) Geiger, T.; Kuster, S.; Yum, J.-H.; Moon, S.-J.; Nazeeruddin, M. K.; Grätzel, M.; Nüesch, F. *Adv. Funct. Mater.* **2009**, *19*, 2720.
- (4) (a) Fan, B.; de Castro, F. A.; Heier, J.; Hany, R.; Nüesch, F. *Org. Electron.* **2010**, *11*, 583. (b) Bouit, P.-A.; Rauh, D.; Neugebauer, S.; Delgado, J. L.; Di Piazza, E.; Rigaut, S.; Maury, O.; Andraud, C.; Dyakonov, V.; Martin, N. *Org. Lett.* **2009**, *11*, 4806.
- (5) (a) Yap, C. C.; Yahaya, M.; Sallen, M. M. *Solar Energy* **2011**, *85*, 95. (b) Benmansour, H.; Castro, F. A.; Nagel, M.; Heier, J.; Hany, R.; Nüesch, F. *Chimia* **2007**, *61*, 787.
- (6) Bouit, P.-A.; Aronica, C.; Toupet, L.; Le Guennic, B.; Andraud, C.; Maury, O. *J. Am. Chem. Soc.* **2010**, *132*, 4328.
- (7) Lacour, J.; Ginglinger, C.; Grivet, C.; Bernardinelli, G. *Angew. Chem. Int. Ed.* **1997**, *36*, 608.
- (8) (a) Malinkiewicz, O.; Lenes, M.; Brine, H.; Bolink, H. J. *RSC Adv.* **2012**, *2*, 3335. (b) Malinkiewicz, O.; Grancha, T.; Molina-Ontoria, A.; Soriano, A.; Brine, H.; Bolink, H. J. *Adv. Energy Mater.* **2013**, *3*, 472. (c) Berner, E.; Jaeger, T.; Lanz, T.; Nüesch, F.; Tisserant, J.-N.; Wicht, G.; Zhang, H.; Hany, R. *Appl. Phys. Lett.* **2013**, *102*, 183903.
- (9) Li, C.-Z.; Matsuo, Y.; Niinomi, T.; Sato, Y.; Nakamura, E. *Chem. Commun.* **2010**, *46*, 8582.

(10) Encinas, C.; Miltsov, S.; Otazo, E.; Rivera, L.; Puyol, M.; Alonso, J. *Dyes Pigments* **2006**, *71*, 28.

(11) IAC is a measure for the intensity of the absorption over the whole absorption band, whereas  $\epsilon$  is a measure for the intensity solely valid at  $\lambda_{\max}$ . See: Shalhoub, G. M. *J. Chem. Educ.* **1997**, *74*, 1317.

(12) Polarity of solvents classified by value of dielectric constant.

(13)  $\text{Alq}_3$  = tris(8-hydroxyquinolino)aluminium

(14) Zhang, H.; Wicht, G.; Gretener, C.; Nagel, M.; Nüesch, F.; Romanyuk, Y.; Tisserant, J.-N.; Hany, R. *Sol. Energy Mater. Sol. Cells* **2013**, *118*, 157.

(15)  $J_{\text{sc}}$  (short circuit current),  $V_{\text{oc}}$  (open circuit voltage), FF (fill factor), and  $\eta$  (efficiency).

(16) (a) Steim, R.; Kogler, F. R.; Brabec, C. J. *J. Mater. Chem.* **2010**, *20*, 2499. (b) Rand, B. P.; Burk, D. P.; Forrest, S. R. *Phys. Rev. B* **2007**, *75*, 115327.

(17) (a) Perez, M. D.; Borek, C.; Forrest, S. R.; Thompson, M. E. *J. Am. Chem. Soc.* **2009**, *131*, 9281. (b) Maurano, A.; Hamilton, R.; Shuttle, C. G.; Ballantyne, A. M.; Nelson, J.; O'Regan, B.; Zhang, W.; McCulloch, I.; Azimi, H.; Morana, M.; Brabec, C. J.; Durrant, J. R. *Adv. Mater.* **2010**, *22*, 4987.